Timing of antiviral treatment initiation is critical to reduce SARS-Cov-2 viral load

Antonio Gonçalves[1], Julie Bertrand[1], Ruian Ke[2], Emmanuelle Comets[1], Xavier de Lamballerie[3], Denis Malvy[4,5], Andrés Pizzorno[6], Olivier Terrier[6], Manuel Rosa Calatrava[6], France Mentré[1], Patrick Smith[7], Alan S Perelson[2] and Jérémie Guedj[1]

[1] Université de Paris, IAME, INSERM, F-75018 Paris, France

[2] Theoretical Biology and Biophysics, Los Alamos National Laboratory, Los Alamos, NM 87545, USA

[3] UMR "Emergence des Pathologies Virales" (EPV: Aix-Marseille University - IRD 190 - Inserm 1207 - EHESP) - Institut Hospitalo-Universitaire Méditerranée Infection, F-13385 Marseille, France

[4] Inserm, UMR 1219, Université de Bordeaux, Bordeaux, France

[5] Centre Hospitalier Universitaire de Bordeaux, Bordeaux, France

[6] Virologie et Pathologie Humaine - VirPath team, Centre International de Recherche en Infectiologie (CIRI), INSERM U1111, CNRS UMR5308, ENS Lyon, Université Claude Bernard Lyon 1, Université de Lyon, Lyon, France.

[7] Certara, Integrated Drug Development, Princeton, NJ, USA

Corresponding author: Jeremie Guedj, jeremie.guedj@inserm.fr

16 rue Henri Huchard, 75018, Paris, France

Conflict of interest

Authors declare no conflict of interest.

Ethical statement

Data were originally provided in Young et al. (doi:10.1001/jama.2020.3204) where "waiver of informed consent for collection of clinical data from infected individuals was granted by the Ministry of Health, Singapore" and "written informed consent was obtained from study participants".

Funding statement

Antonio Gonçalves was funded by a grant from Roche Pharmaceutical Research and Early Development.

Portions of this work were done under the auspices of the U.S. Department of Energy under contract 89233218CNA000001. We also gratefully acknowledge the support of the U.S. Department of Energy through the LANL/LDRD Program for this work as well as N.I.H. grants R01 AI028433, R01 OD011095, R01 AI078881 and P01 AI131365 (ASP).

Abstract (word count: 100/100)

We modeled the viral dynamics of 13 untreated patients infected with SARS-CoV-2 to infer viral growth parameters and predict the effects of antiviral treatments. In order to reduce peak viral load by more than 2 logs, drug efficacy needs to be greater than 80% if treatment is administered after symptom onset; an efficacy of 50% could be sufficient if treatment is initiated before symptom onset. Given their pharmacokinetic/pharmacodynamic properties, current investigated drugs may be in a range of 20-70% efficacy. They may help control virus if administered very early, but may not have a major effect in severe patients.

Keywords

SARS-CoV-2; COVID-19; timing for treatment initiation; hydroxychloroquine; interferon-beta-1a; lopinavir/ritonavir; viral dynamics; acute infection; simulations

Main text (word count: 1,991/2,000)

Background

The outbreak of severe acute respiratory syndrome coronavirus 2 (SARS-CoV-2), which originated in Wuhan, China, has become a global pandemic. By March 29, 2020, this virus had infected more than 700,000 people worldwide and caused more than 30,000 deaths. Despite the unprecedented mobilization of the clinical and scientific community, the development and large scale implementation of new antiviral drugs or vaccines will take months or more. To readily propose a first line of defense and combat the virus in hospitalized patients, the World Health Organization relies on already existing drugs ("repurposed") that are immediately available in large quantities and have a good safety profile. In coordination with other European institutions, France is implementing a randomized clinical trial in hospitalized patients ("DisCoVery", NCT04315948) comparing the efficacy of lopinavir/ritonavir ± IFN-β-1a, remdesivir and hydroxychloroquine. Given the very limited knowledge of the host/pathogen interaction the clinical efficacy of treatment strategies using these drugs is largely unknown and could be limited [1].

Fitting mathematical models of viral dynamics to *in vivo* data can provide estimates of parameters driving viral replication. Such models can then be used to predict the needed efficacy of treatments and to optimize their use [2]. By combining these predictions with the expected drug concentrations and EC_{50} of drug candidates, one can anticipate the effects of various dosing regimens (doses, timing of treatment initiation) on viral load dynamics.

Methods

Data used for fitting

We used published data from 13 untreated patients infected with SARS-CoV-2 that were followed in 4 Singapore hospitals [3]. Patients were hospitalized in median at day 3 after onset of symptoms (range: 1-10) and had a median symptomatic period of 12 days (range: 5-

24). Viral loads in nasopharyngeal swabs were measured by real time reverse transcriptase polymerase chain reaction (RT PCR, lower limit of quantification: 38 cycles, CT) at multiple time points with an observed peak of viral load at day 5 post onset of symptoms (range: 2-27 days). Data presented in CT were transformed to log10 copies/mL using a published relationship in Zou et al. [4] and the model was fit to the log10 viral load. Of note, the transformation from CT to log 10 copies/mL does not affect the estimates of parameters of interest, in particular R_0 and the death rate of productively infected cells. Time since infection was assumed to be 5 days before the onset of symptoms [5]. In a sensitivity analysis, we also examined values of 2 and 10 days.

Model

Viral dynamics was fitted using a target cell limited model with an eclipse phase

$$\frac{dT}{dt} = -\beta VT$$

$$\frac{dI_1}{dt} = \beta VT - kI_1 \qquad \text{Equation 1}$$

$$\frac{dI_2}{dt} = kI_1 - \delta I_2$$

$$\frac{dV}{dt} = pI - cV$$

The model considers three populations of cells: target cells, T, infected cells in the eclipse phase, I_1, and productively infected cells, I_2. Given the timescale of the infection, we neglect target cell proliferation and natural death, and we focused on the process of cell depletion by virus infection. We assumed target cells become infected with rate constant β. After an average time of $1/k$, these cells start producing virus and are cleared with per capita rate δ. Virions are released from productively infected cells I_2 at rate p per cell and are cleared from the circulation at per capita rate c. Based on this model, the basic reproduction number,

R_0, the average number of cells infected by a single infected cell at the beginning of the infection, is [6]

$$R_0 = \frac{p\beta T_0}{\delta c}. \qquad \text{Equation 2}$$

We assumed that the target cell concentration is 1.33×10^7 cells/mL. Assuming a 30 mL volume for the nasopharynx [7] this gives a total number of target cells of 4×10^8 nasopharyngeal cells [8]. Following what was found in other viral infections, including acute infection [6], the clearance rate of virus was assumed to be fast and equal to 10 d^{-1}. We also performed a sensitivity analysis assuming c= 5 and 20 d^{-1} and found that the estimate of δ remained unchanged and the estimate of R_0 varied from 12.4 to 15.5.

Model building strategy

Because not all parameters can be identified when only viral load data are available, the model was successively fitted with different values of k={1, 3 ,5}d^{-1} and V_0={10^{-3}, 10^{-2}, 10^{-1}} copies/mL [6]**.** Parameters were estimated in a non-linear mixed-effect modeling framework using the SAEM algorithm implemented in Monolix (www.lixoft.com). The model providing the best description of the data was used for the predictions and the individual data fitting, and model averaging was used to correct for the model uncertainty when calculating confidence intervals of estimated parameters [9].

Predicting the effects of treatment according to the antiviral efficacy and the timing treatment of initiation

We assumed that antivirals with a constant effectiveness ε could reduce R_0 by a factor (1-ε), with ε taking values from 50% to 99% in Equation 2. We considered different timing of treatment initiation, from the time of infection to 3 days after the symptom onset. For each treatment strategy, we calculated the reduction in viral load at the peak of infection in the

absence of treatment, i.e., 5 days after symptom onset. The model providing the best description of the data was used for the simulations, and sensitivity analyses were conducted to evaluate the results obtained with different assumptions regarding the delay between time of infection and time of symptom onset either 2 or 10 days (Supplemental information, Fig S1 and S2).

PK/PD drug properties of lopinavir/ritonavir, hydroxychloroquine and IFN-β-1a

We relied on the literature to find PK population parameters of lopinavir/ritonavir [10], hydroxychloroquine [11], and IFN-β-1a [12] as well as reported EC_{50} values *in vitro* (see Table 1). For lopinavir, EC_{50} Vero E6 cells were infected by SARS-CoV-2 (strain BetaCoV/France/IDF0571/2020) at a MOI of 0.01 and treated with several concentrations of lopinavir one hour after infection. Supernatant samples were collected at 48 and 72 hour post infection. Relative quantification of viral genome was performed by RT-qPCR from RNA extracted using QIAamp viral RNA Mini Kit (Qiagen). IC50 values of lopinavir (5.246 μM and 4.941 μM at 48 and 72 hours post infection, respectively) were calculated from dose-response curve using a four-parameter logistic regression model. CC50 were determined using a MTS viability assay in Vero E6 cells treated by a large range of lopinavir concentrations. No published results on remdesivir pharmacokinetics was available at the time of this publication. We then simulated 100 PK profiles according to the estimated distribution and we calculated for each simulated individual the mean inhibitory coefficient during the first week of treatment, to anticipate their effect on peak viral load. For comparison purposes, we based the analysis on blood concentrations and did not adjust for plasma protein binding when computing efficacy.

Table 1: PK/PD properties of candidate antiviral drugs. We assume that the total blood concentrations were the driver of efficacy, and we did not consider intracellular metabolites or free drug concentrations

Drug	PK parameter	EC_{50} (μM)	Dosing regimen D0-D7	$\overline{\varepsilon} = \frac{1}{7} \times \int_0^7 \frac{C(u)}{C(u) + EC_{50}} du$
Lopinavir/ritonavir	Wang et al. [10]	5.2 (unpublished)	400/100 BID	66%
Hydroxychloroquine	Morita et al [11]	0.72 [13]	400 mg BID at D0, followed by 400 mg QD	33%
IFN-β-1a	Hu et al. [12]	175 IU/mL [14]	12 MIU at D0, D2, D5	18%

Results

Here we used a "target-cell limited" model with an eclipse phase [8] given by Eq. (1) to characterize the viral load dynamics of 13 hospitalized patients in Singapore for which data obtained from frequent nasopharyngeal swabs were available [3] (Fig S3). Because this model needs to incorporate a date of infection, an incubation period of 5 days was used to project the most plausible date of infection in each patient [5] (see Supplemental Information for a sensitivity analysis). The model fit the data well (Fig S3); using a model averaging approach to take into account model uncertainty [9], the within-host basic reproductive number, R_0, was found equal to 12.9 ($CI_{95\%}$=[2.3-46.7]), and the death rate of productively infected cells was estimated as 0.54 d^{-1} ($CI_{95\%}$=[0.21-0.87]), corresponding to a median half-life of 1.3 days (See Supplemental information Fig S4 and Table S1). In influenza A, another respiratory infectious disease, estimates of the within host R_0 varied greatly, but the half-life of infected cells was shorter than 10 hours (see more details in [15]), suggesting a faster clearance of influenza infected cells than SARS-CoV-2.

These numbers also inform us both on the time to initiate antiviral treatment, and the level of efficacy that needs to be achieved to reduce viral load [6]. As limited information is available on the mechanisms leading to viral clearance, and how they may be modulated by treatment, we used our model to predict the effects of treatment at day 5 post symptoms, which corresponds to the time the viral load tends to peak in the absence of treatment [3]. We considered a simple case where the drug effectiveness is assumed to be constant after therapy initiation (see methods) and we calculated the minimal efficacy that would be needed to generate more than 2 logs of viral decline at peak viral load in the 13 studied patients (Fig. 1). As predicted by viral kinetic modeling theory [2], we found that the impact of treatment on peak viral load is inversely correlated with the time of treatment initiation. For a putative treatment initiated at the time of infection, symptom onset, or 3 days post symptom onset, a median efficacy of at least 60, 90 and 99% in reducing viral replication would be needed, respectively, to generate more than 2 log of decline in the peak viral load (Fig. 1).

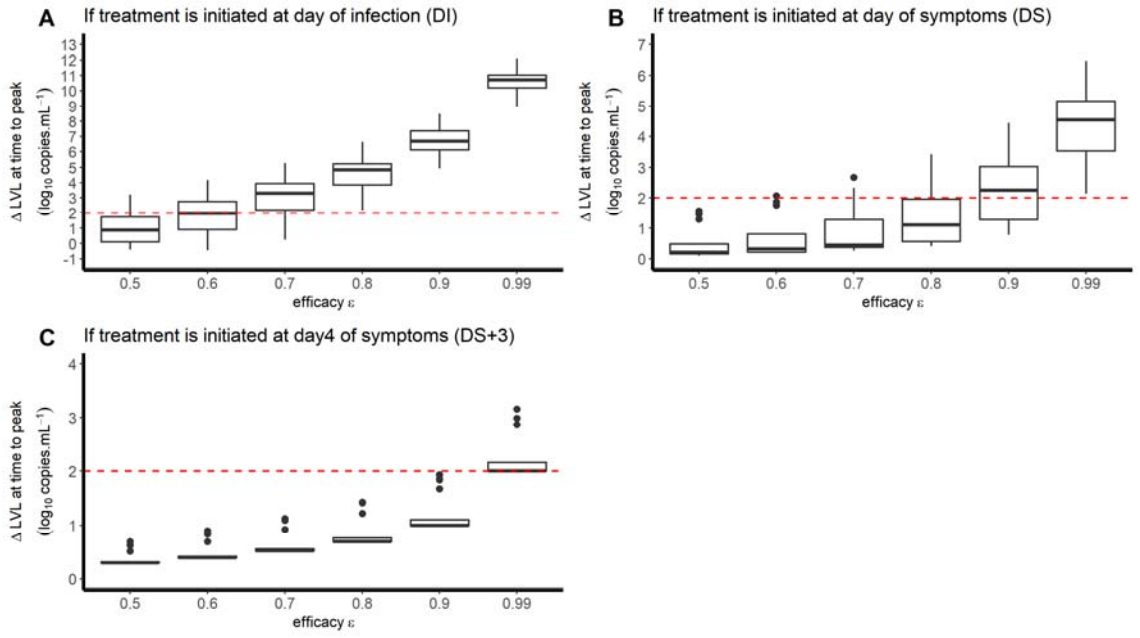

Figure 1: Reduction in viral load at day 5 post symptom onset according to the level of antiviral effectiveness and the timing of treatment initiation (A: at time of infection; B: at time of symptom onset; C: 3days after symptom onset). We assumed an incubation period of 5 days

How do these levels of effectiveness compare with the antiviral drugs that are currently being investigated? To study this question, we assumed that the treatment antiviral effectiveness at time *t* after treatment initiation, $\varepsilon(t)$, was related to the plasma total drug concentration, *C(t)*: $\varepsilon(t) = \frac{C(t)}{C(t)+EC_{50}}$ and the mean antiviral effectiveness during the first 7 days of treatment is given by $\overline{\varepsilon} = \frac{1}{7} \times \int_0^7 \frac{C(u)}{C(u)+EC_{50}} du$. Given their pharmacokinetic and pharmacodynamic properties (Table 1), we calculated a mean antiviral efficacy of up to 66% for lopinavir/ritonavir, 18% for IFN-β-1a, and 33% for hydroxychloroquine. Given these estimates, these compounds are unlikely to have a dramatic effect on peak viral load if administered after the onset of symptoms. In fact, the effective concentrations will presumably be lower in patients, as relevant drug may be further limited by protein binding (in particular for lopinavir, which has a protein binding rate > 98%) or capability to penetrate respiratory compartments, which is not well characterized. Importantly, levels of antiviral efficacy of ~50% could nonetheless be relevant in a prophylactic setting, before symptom onset, to reduce viral replication in the upper respiratory tract and reduce the risk of large infiltration to the lung before an effective immune response is mounted to clear virus [2] Note, above we calculated the effectiveness of drugs administered in monotherapy for their usual dosing regimen. We also did not consider drugs that could directly target infected cells and lead to their elimination, such as some monoclonal antibodies.

Discussion

Overall our results emphasize that the PK/PD properties of lopinavir/ritonavir, IFN-β-1a and hydroxychloroquine make them unlikely to have a dramatic impact on viral load kinetics in the nasopharynx if they are administered after symptom onset. Given this, it is possible that continued viral replication in the presence of drug will select for drug resistant mutations as has been seen with other RNA viruses [7], although coronaviruses are unusual in that they

appear to have low mutation rates due to RNA proofreading capability. Drug combination therapy and more aggressive dosing, including consideration of loading doses to rapidly achieve therapeutic exposures, may be beneficial to maximize efficacy of these repurposed antiviral agents. However, they may be relevant in pre- or post-exposure prophylaxis administration to reduce viral replication and hence the risk of disease progression.

References

1. Cao B, Wang Y, Wen D, et al. A Trial of Lopinavir–Ritonavir in Adults Hospitalized with Severe Covid-19. N Engl J Med. **2020**; :NEJMoa2001282.

2. Friberg LE, Guedj J. Acute bacterial or viral infection—What's the difference? A perspective from PKPD modellers. Clin Microbiol Infect. **2019**; :S1198743X19306639.

3. Young BE, Ong SWX, Kalimuddin S, et al. Epidemiologic Features and Clinical Course of Patients Infected With SARS-CoV-2 in Singapore. JAMA [Internet]. **2020** [cited 2020 Mar 29]; . Available from: https://jamanetwork.com/journals/jama/fullarticle/2762688

4. Zou L, Ruan F, Huang M, et al. SARS-CoV-2 Viral Load in Upper Respiratory Specimens of Infected Patients. N Engl J Med. **2020**; 382(12):1177–1179.

5. Lauer SA, Grantz KH, Bi Q, et al. The Incubation Period of Coronavirus Disease 2019 (COVID-19) From Publicly Reported Confirmed Cases: Estimation and Application. Ann Intern Med [Internet]. **2020** [cited 2020 Mar 29]; . Available from: https://annals.org/aim/fullarticle/2762808/incubation-period-coronavirus-disease-2019-covid-19-from-publicly-reported

6. Best K, Guedj J, Madelain V, et al. Zika plasma viral dynamics in nonhuman primates provides insights into early infection and antiviral strategies. Proc Natl Acad Sci. **2017**; 114(33):8847–8852.

7. Perelson AS, Rong L, Hayden FG. Combination Antiviral Therapy for Influenza: Predictions From Modeling of Human Infections. J Infect Dis. **2012**; 205(11):1642–1645.

8. Baccam P, Beauchemin C, Macken CA, Hayden FG, Perelson AS. Kinetics of influenza A virus infection in humans. J Virol. **2006**; 80(15):7590–7599.

9. Gonçalves A, Mentré F, Lemenuel-Diot A, Guedj J. Model Averaging in Viral Dynamic Models. AAPS J. **2020**; 22(2):48.

10. Wang K, D'Argenio DZ, Acosta EP, et al. Integrated Population Pharmacokinetic/Viral Dynamic Modelling of Lopinavir/Ritonavir in HIV-1 Treatment-Naïve Patients. Clin Pharmacokinet. **2014**; 53(4):361–371.

11. Morita S, Takahashi T, Yoshida Y, Yokota N. Population Pharmacokinetics of Hydroxychloroquine in Japanese Patients With Cutaneous or Systemic Lupus Erythematosus: Ther Drug Monit. **2016**; 38(2):259–267.

12. Hu X, Shang S, Nestorov I, et al. COMPARE: Pharmacokinetic profiles of subcutaneous peginterferon beta-1a and subcutaneous interferon beta-1a over 2 weeks in healthy subjects: Pharmacokinetics of peginterferon beta-1a and s.c. interferon beta-1a. Br J Clin Pharmacol. **2016**; 82(2):380–388.

13. Yao X, Ye F, Zhang M, et al. In Vitro Antiviral Activity and Projection of Optimized Dosing Design of Hydroxychloroquine for the Treatment of Severe Acute Respiratory Syndrome Coronavirus 2 (SARS-CoV-2). Clin Infect Dis. **2020**; :ciaa237.

14. Sheahan TP, Sims AC, Leist SR, et al. Comparative therapeutic efficacy of remdesivir and combination lopinavir, ritonavir, and interferon beta against MERS-CoV. Nat Commun. **2020**; 11(1):222.

15. Smith AM. Host-pathogen kinetics during influenza infection and coinfection: insights from predictive modeling. Immunol Rev. **2018**; 285(1):97–112.

Table 1 PK/PD properties of candidate antiviral drugs. We assume that the total blood concentrations were the driver of efficacy, and we did not consider intracellular metabolites or free drug concentrations

Drug	PK parameter	EC_{50} (μM)	Dosing regimen D0-D7	$\overline{\varepsilon}(t) = \frac{1}{7} \times \int_0^7 \frac{C(u)}{C(u) + EC_{50}} du$
Lopinavir/ritonavir	Wang et al.[11]	5.2 (unpublished)	400/100 BID	66%
Hydroxychloroquine	Morita et al[12]	0.72[14]	400 mg BID at D0, followed by 400 mg QD	33%
IFN-β-1a	Hu et al.[13]	175 IU/mL[15]	12 MIU at D0, D2, D5	18%

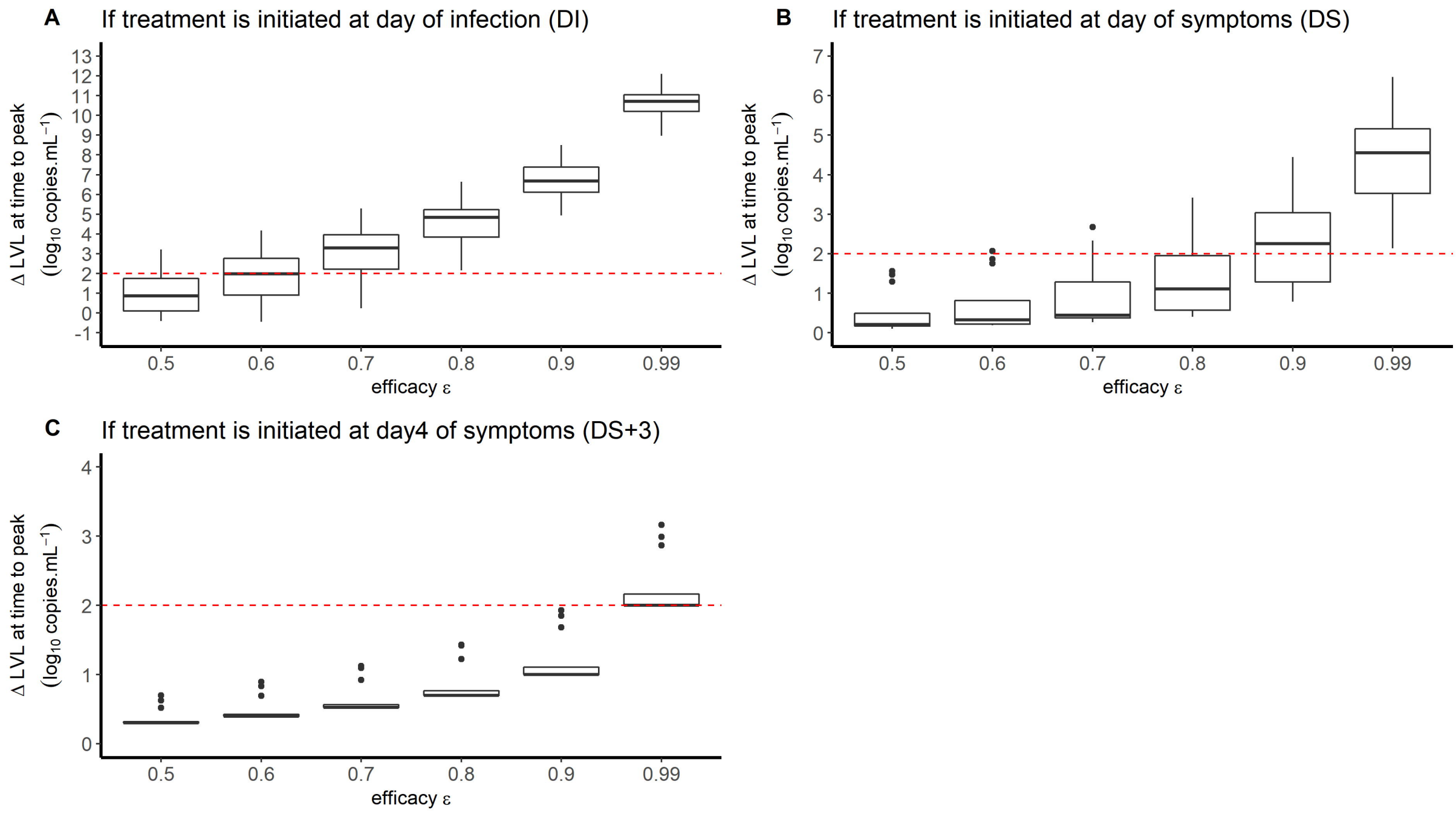
A
If treatment is initiated at day of infection (DI)
Δ LVL at time to peak
(log10 copies.mL−1)
13
12
11
10
9
8
7
6
5
4
3
2
1
0
-1
0.5
0.6
0.7
0.8
0.9
0.99
efficacy ε
B
If treatment is initiated at day of symptoms (DS)
Δ LVL at time to peak
(log10 copies.mL−1)
7
6
5
4
3
2
1
0
0.5
0.6
0.7
0.8
0.9
0.99
efficacy ε
C
If treatment is initiated at day4 of symptoms (DS+3)
Δ LVL at time to peak
(log10 copies.mL−1)
4
3
2
1
0
0.5
0.6
0.7
0.8
0.9
0.99
efficacy ε